Analysis of Balloon Trajectory Prediction Methods

Ethan E. Harstad*

Iowa State University, Ames, IA

Most balloon trajectory prediction algorithms date back to when computational time was expensive and therefore use many simplifications. This paper presents a discussion of these simplifications, their effects, and the efforts made to increase the accuracy of trajectory predictions in the HABtk balloon flight prediction software.

Nomenclature

$\mathbf{v_a}, \mathbf{v_b}$	Velocity of the atmosphere and balloon
μ	Dynamic viscosity
ρ_a	Density of ambient air
ρ_g	Density of lifting gas
C_D	Drag coefficient of the balloon
C_m	Added mass coefficient
Re	Reynolds number
V_b	Balloon volume

I. Introduction

Accurate balloon trajectory predictions become increasingly important with increases in mission duration, payload expense, and risk. Because any error in the prediction model accumulates over time, extended duration flights are particularly difficult to predict accurately. The risk of hardware failure and the rising cost of payloads similarly necessitates the most accurate prediction possible.

Accurate predictions also allow new experimental techniques. If the expected ascent rate can accurately be determined (either a priori or from recorded data) the vertical motion of the air column can be determined.[1] Increased accuracy of lateral predictions makes techniques such as trajectory match sampling much more useful and allows methods such as choosing a launch site to land the balloon in a given area.

The majority of trajectory prediction algorithms date back to when computing time was expensive and advanced algorithms were not practical. This lead to simplifications such as constant ascent rate which have no theoretical basis outside of convenience.

II. Theoretical Background

Accurately predicting the flight of high altitude balloons requires accurately representing the forces acting on the balloon system. The prediction is solved by integrating the equations of motion from given initial conditions. Therefore any error in the estimation of forces (and most initial conditions) is compounded with time.

The primary forces acting on the balloon system are buoyancy, gravity, and aerodynamic forces. These forces can be decomposed into horizontal and vertical components which are essentially decoupled as will

---

*Student Engineer, Aerospace Engineering

be shown later. It has been seen via experiment that the payload moves in relation to the balloon and the envelope of the balloon deforms but the effects of these motions can be ignored as they are essentially zero mean random noise.

A.   Horizontal Motion

The primary force driving the horizontal motion of the balloon system is drag created by relative motion between the atmosphere and the balloon system. Most prediction algorithms assume that the balloon system's horizontal motion exactly matches the horizontal motion of the atmosphere. This assumption is essentially correct for lightly loaded balloons, especially at lower altitudes, but becomes less accurate at higher altitudes. When subjected to a $2m/s$ step change in wind velocity, a lightly loaded radiosonde balloon requires 20 seconds to catch up to the wind at $15km$, this increases to 40 seconds at $30km$. At the opposite extreme, a $1000kg$ zero-pressure balloon requires 3 minutes at $15km$, 7 minutes at $30km$, and 15 minutes at $45km$.[2] Assuming a nominal ascent rate of $5m/s$, the radiosonde will climb $200m$ and the zero-pressure balloon over $2km$. This assumption produces passable results if there are no shear layers in the atmosphere thinner than the response time of the balloon.

The physics of the horizontal motion of the balloon are essentially captured in the following equations.

$$F_D = m_t \frac{\mathbf{dv}}{dt} \tag{1}$$

$$F_D = \frac{1}{2}\rho_a \left(\mathbf{v_a} - \mathbf{v_b}\right)^2 A_b C_D \tag{2}$$

$$m_t = m_p + m_b + m_g + C_m \rho_a V_b \tag{3}$$

$$m_g = V_b \rho_g \tag{4}$$

The force acting on the balloon is a function of the relative velocity of the balloon and atmosphere, the ambient density, the size of the balloon, and the drag coefficient. The drag coefficient also varies with many of these parameters and is discussed in section C. It is important to note that the mass of the system is the total mass, including the lifting gas, plus the added mass ($C_m = 0.5$ for spherical balloons) of the air that is affected by the motion of the balloon.[3] This means that the effective mass of the balloon system also varies with altitude.

A simulation was run comparing the response time and the error created by the equilibrium assumption for a 1200 gram latex balloon with a $5kg$ payload and $6.8kg$ of neck lift. The graph of the response time vs altitude in shown in figure A. The error resulting from the equilibrium assumption shows similar character to the response time, increasing from $5m$ to approximately $30m$ at $35km$. It is left to the reader to determine if this error is acceptable for their application.

B.   Vertical Motion

The vertical motion of the balloon is a result of the lift, drag and gravitational forces on the balloon system. The lift of the balloon is a function of the density of the lifting gas and the volume of the balloon. The density can be regarded as constant over the volume of the balloon for the typical size of latex balloons but pressure and temperature gradients must be account for in larger balloons. The basic governing equations are summarized below.
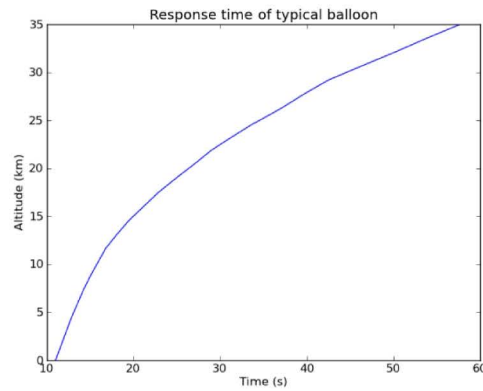
$$L = D + W \tag{5}$$

$$V_b(\rho_a - \rho_g)g = \frac{1}{2}\rho_a v_z^2 A_b C_D + (m_b + m_p)g \tag{6}$$

$$\frac{4}{3}\pi r^3(\rho_a - \rho_g)g = \frac{1}{2}\rho_a v_z^2 \pi r^2 C_D + (m_b + m_p)g \tag{7}$$

By treating the lifting gas as an ideal gas, the density may be solved for by using the ideal gas law. One important effect typically that is typically ignored is the overpressure created by the balloon envelope. This

Figure 1. Response time to unit step wind

pressure can be computed by the Gent hyper-elastic model.[4] The pressure created by the balloon is typically on the order of 100 to 200 pascals and is therefore safe to ignore at lower altitudes, but becomes increasingly significant as ambient pressure decreases. This can be seen in figure B.

Figure 2. Effect of membrane pressure on balloon radius
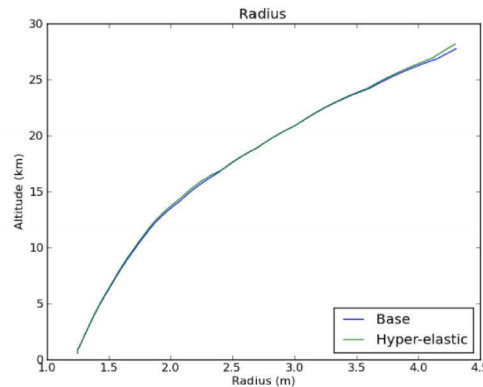
A simulation was run against data collected from a previous flight and the results are summarized in figure B. As can be seen, the constant ascent rate assumption used in many models is not very accurate, even if the predicted rate more closely matched the observed value. The constant drag coefficient (CDP) model also diverges from the observed data. The character of the variable drag coefficient (VDP) model most closely matches the observed ascent profile and this drag behavior is discussed in section C.
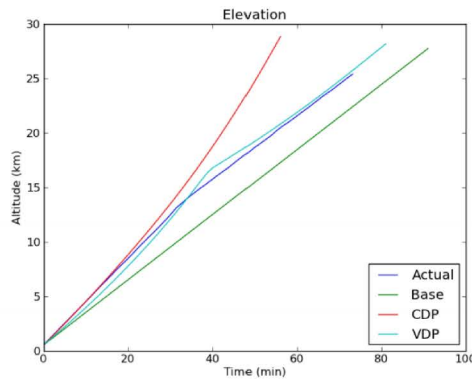
C. Drag

In order to predict the drag behavior of balloons, a spherical approximation is used. The drag coefficient of a sphere is a function of the Reynolds number of the flow:

$$Re = \frac{\rho v L}{\mu} \qquad (8)$$

Figure 3. Elevation profiles of various algorithms

where μ is the dynamic viscosity of the fluid which is a function of temperature. Spheres in particular present a complex drag behavior that is primarily due to the transition of the boundary layer from turbulent to laminar which causes the separation point to advance on the sphere and subsequently widens the wake and increases drag.[5] It has recently been shown that due to the nature of the drag crisis, the drag of a spheroid is also highly dependent on the turbulence intensity of the fluid.[6] The effect of increased turbulence is to decrease the critical Reynolds number and decrease the slope of the transition region. Further studies have compared the drag of oblate spheroids and shown that they display largely the same behavior but with generally higher values.[7]

A simulation was run against data from a previous balloon flight using a scaled and shifted spherical drag model. The results are summarized in figure C. As discussed previously, the constant ascent rate and constant drag profiles are largely false. The variable drag model used here is scaled and shifted from the ideal sphere model and largely presents the correct profile. The scaling factor used here is 3 and is justified by the previous discussion of oblate spheroid drag.

Figure 4. Ascent rates of various algorithms
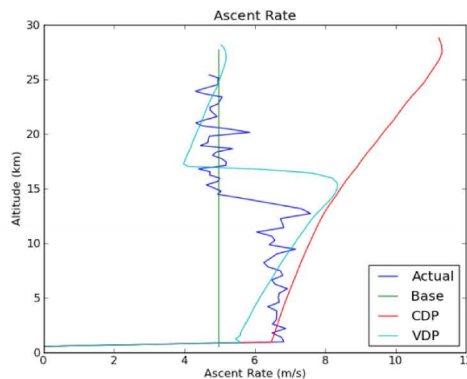
There are additional aerodynamic effects that contribute to drag that have not been significantly studied. In wind tunnel experiments, a body is typically held rigidly in the flow and therefore has an apparent mass

approaching infinity. This limits the effect that vortices can have on the drag of the body. A balloon has a much lower mass and the effect of a trailing or shedding vortex could be quite significant. For these reasons the author is working with the National Near Space Association and Aerodyne Labs to establish a data repository for high altitude balloon telemetry. This repository is planned to be open to the public and will automatically be used to improve the drag models used for the prediction of latex balloon flights.

III. Tracking

The prediction model described here is equally valid for real-time tracking of a balloon in flight. Very accurate estimations of the landing zone can be obtained by updating the initial conditions used for the prediction with values derived from the observed motion of the balloon. The author is implementing this in the freely available HABtk (High Altitude Balloon tool kit).

Two a priori values that greatly benefit from modification based on observed data are the ascent and descent rates of the system. It can be difficult to fill the balloon to the desired lift (and difficult even to measure in windy environments) and it is very difficult to predict the descent rate accurately due to variances in the deployment of the parachute. To improve the estimate of ascent rate, an iterative algorithm is used to compute the required lift to produced the observed average ascent rate. The computed lift can then be used as an initial value to obtain a more accurate prediction from the current balloon position. Similarly the descent rate estimation can be improved by measuring the observed descent rate and directly computing the required parachute area or drag coefficient. The results of running this adaptive method on telemetry from an earlier flight are summarized in figure III.

The wind speed can also be extracted from the ascent profile using the prediction model and used to improve the estimation of wind speed and direction. One trivial method is to simply store the observed values for wind speed and direction and use the stored values for the remaining prediction. The downside to this trivial method is that the observed values are only useful during the descent prediction. A more advanced method could use the difference between the initial wind forecast and the observed values to extrapolate wind speeds above the current altitude of the balloon. This would most likely involve a significant data set and possibly a more advanced atmospheric model. The author has chosen instead to pursue a model based on the extended Kalman filter (EKF). Two a priori profiles are used, one profile from before the flight and one after. The observed values are used to evolve the wind profile interpolated from the a priori values using the EKF. More test cases are needed to evaluate and improve the performance of this model.

The adaptive methods described above were applied to data collected from a previous flight and summarized in figure III. Naive predictions are utilizing a priori data only while adaptive predictions attempt to compensate for any inaccuracies of the a priori data. The one dimensional algorithm only attempts to correct for ascent and descent rates while the two dimensional algorithm only attempts to correct for wind variances. The three dimensional algorithm combines these methods. This graph is only a sampling of the algorithm and the relative accuracy of the lower order methods is purely coincidental. As can be seen from the graph, there is still no reliable method to predict an early burst. The author hopes that with a larger data set a pre-burst behavioral trait can be identified to improve the prediction of burst altitude.

IV. Conclusion

The preceding discussion has shown that there are large gains to be had from more advanced prediction algorithms. Increased accuracy allows new experimental methods and increases the reliability and safety of high altitude balloon missions. With the increased popularity of high altitude ballooning and ever increasing air traffic, balloonists need to do everything that they can to increase the safety of their missions.

It has also been shown that current models have a long ways to go. More accurate drag models are needed and can be achieved by gathering more data. Other things such as the effects of thermal conduction and radiation will require more experimental and theoretical analysis.

Figure 5. Results of various adaptive tracking algorithms
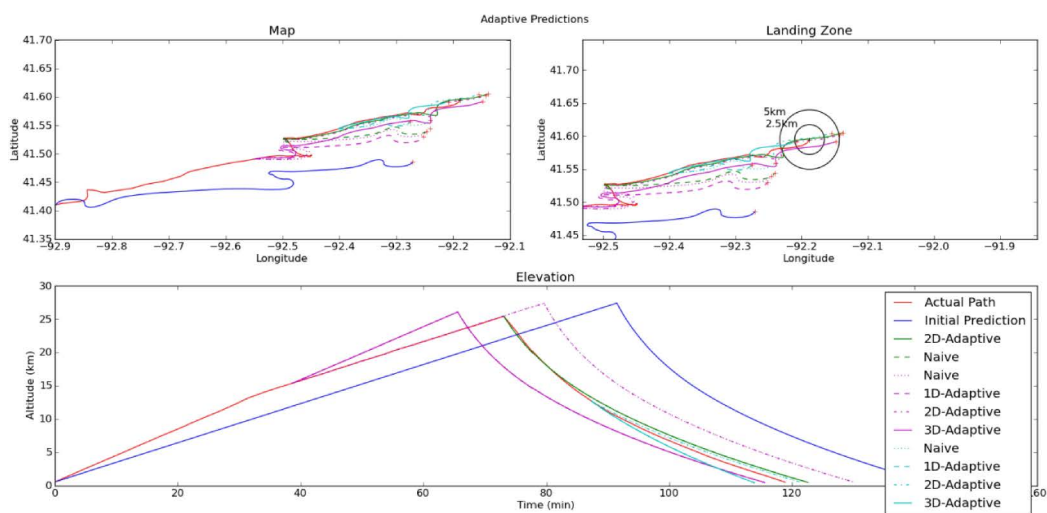
References

[1]Gallice, A., Wienhold, F. G., Hoyle, C. R., Immler, F., and Peter, T., "Modeling the ascent of sounding balloons: derivation of the vertical air motion," *Atmospheric Measurement Techniques Discussions*, Vol. 4, No. 3, 2011, pp. 3965–4012.

[2]Yajima, N., Imamura, T., Izutsu, N., and Abe, T., "Engineering Fundamentals of Balloons," *Scientific Ballooning*, Springer New York, 2009, pp. 15–75.

[3]Anderson, W., Shah, G., and Park, J., "Added mass of high-altitude balloons," *Journal of Aircraft*, Vol. 32, No. 2, 1995, pp. 285–289.

[4]Kanner, L. M. and Horgan, C. O., "Elastic instabilities for strain-stiffening rubber-like spherical and cylindrical thin shells under inflation," *International Journal of Non-Linear Mechanics*, Vol. 42, No. 2, 2007, pp. 204 – 215, ¡ce:title¿Special Issue in Honour of Dr Ronald S. Rivlin¡/ce:title¿.

[5]Vennard, J., *Elementary fluid mechanics*, Wiley, 4th ed., 1961.

[6]Son, K., Choi, J., Jeon, W.-P., and Choi, H., "Effect of free-stream turbulence on the flow over a sphere," *Physics of Fluids*, Vol. 22, No. 4, 2010, pp. 045101.

[7]Loth, E., "Drag of non-spherical solid particles of regular and irregular shape," *Powder Technology*, Vol. 182, No. 3, 2008, pp. 342–353.